Thermochimica Acta, 241 (1994) 171–189
Elsevier Science B.V., Amsterdam
SSDI 0040-6031(93)01679-B

Non-isothermal kinetics of dehydration and decomposition of nickel chloride hydrate

S.B. Kanungo* and S.K. Mishra

Regional Research Laboratory, Bhubaneswar-751 013, Orissa, India

(Received 6 September 1993; accepted 13 December 1993)

Abstract

The dehydration and decomposition behaviour of nickel chloride hydrate has been studied by a non-isothermal method with different experimental conditions such as heating rate, sample size, inert gas flow, etc. Kinetic parameters for the different steps of the dehydration and decomposition have been determined from DTA and TG curves using both model-independent and model-dependent methods of data analysis. The results are critically examined to determine meaningful kinetic parameters which, however, sometimes differ from those derived isothermally.

INTRODUCTION

In our preceding paper [1], we reported kinetic parameters for the isothermal dehydration of nickel and cobalt chloride hydrates. While the first major dehydration step for nickel chloride hydrate follows a second-order rate law, in the case of cobalt chloride hydrate a complex process of diffusion is found to be operative up to the formation of the dihydrate. The final stage of dehydration for both salts follows a one-dimensional diffusion or parabolic rate law. However, an unusually low activation energy value for the initial dehydration of the two hydrated salts suggests that despite differences in the mechanistic model, some subtle similarity exists which is possibly obscured by the large difference in their rates of dehydration. Because TGA curves can provide a better resolution of the different steps of a reaction, kinetic analysis of such curves sometimes yields a better insight into the mechanism of any thermal process than can be obtained from an isothermal method. In this paper, the results of the non-isothermal kinetic analysis of the thermal dehydration and decomposition of nickel chloride hydrate are reported.

* Corresponding author.

EXPERIMENTAL

Materials

Both undried and partially dried nickel chloride hydrates containing different (7.55–5.53) moles of water per mole of nickel chloride were used in the present investigation.

Methods

Thermal analysis under dynamic or non-isothermal conditions was carried out using two different pieces of equipment: the NETZSCH model STA-409 (Germany) and the Shimadzu model DT-40 with micro-processor (Japan). Whereas in the former a cylindrical platinum sample holder having a capacity to hold as much as 150 mg of sample was used, in the latter an alumina micro-crucible with a maximum capacity of 18–20 mg was used. Therefore, the effect of variation of sample size was mostly carried out in the former equipment. However, the effect of heating rate was investigated using both types of apparatus. Calcined (1200°C) α-Al_2O_3 was used as reference in both. Dry nitrogen at a flow rate of 50 ml min^{-1} was passed for a few selected experiments.

RESULTS AND DISCUSSION

The effect of various experimental variables on the nature of the thermograms of the samples is briefly discussed below before embarking upon the kinetic analysis. For a highly hygroscopic salt which melts before dehydration and decomposition, the effect of grain size cannot be studied meaningfully.

Effect of heating rate

Figures 1 and 2 illustrate the effect of heating rate on the TA curves of nickel chloride hydrate obtained from the two different pieces of equipment. The relevant data are given in Table 1. (It is not the intention of this work to judge the suitability of one apparatus over the other. The purpose is to demonstrate how the thermogram of a substance varies with the equipment used.) It can be seen that the results obtained from the STA-409 exhibit a more consistent variation with increase in heating rate than those from the DT-40. Although the DTA peak temperatures for the initial melting appear at approximately the same temperature for both apparatus, the first stage of dehydration begins at a lower temperature in the DT-40 than that in STA-409. The TGA data obtained from both confirm the loss of about 4 moles of water in the first step of dehydration. The appearance of a new

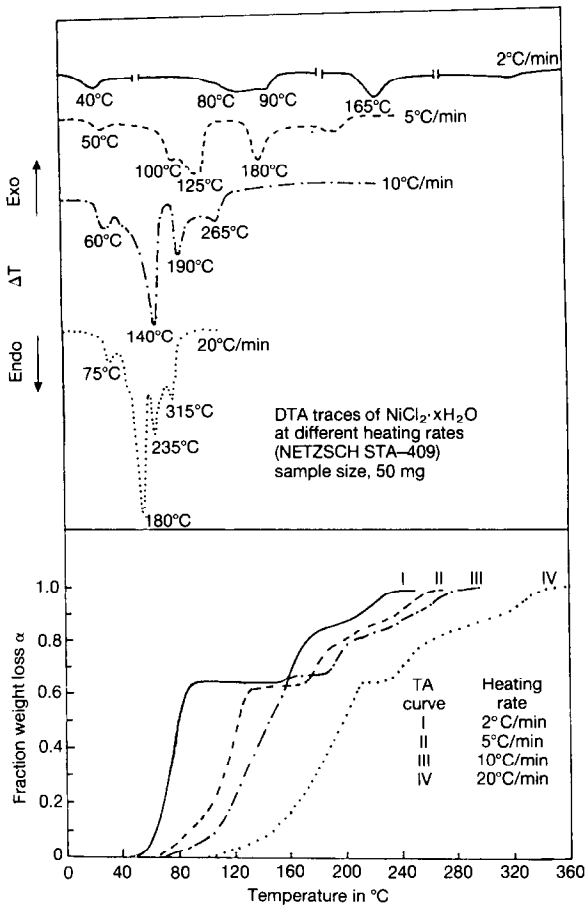

Fig. 1. Thermograms of $NiCl_2 \cdot xH_2O$ obtained using a NETZSCH model STA-409 at different heating rates.

crystalline phase, the dihydrate, appears as a prominent endothermic peak in the DT-40, whereas this peak is conspicuously absent in the thermograms from the STA-409. For the second stage of dehydration, the DT-40 records more loss of water at a higher temperature range than the STA-409. However, the DTA peak temperature for this stage of water loss appears 15–20°C higher in the STA-409. A similar observation can be made for the third stage of water loss. While this last stage of water loss is clearly discernible in the TG traces obtained from the STA-409, this appears as a continuous curve in the DT-40. However, the two stages can be delineated by the sharp DTA peak for this stage of dehydration in the DT-40.

Effect of sample size

Because the nature of the TA curves does not undergo any major change with sample size, except for a shifting of the temperatures, only the relevant

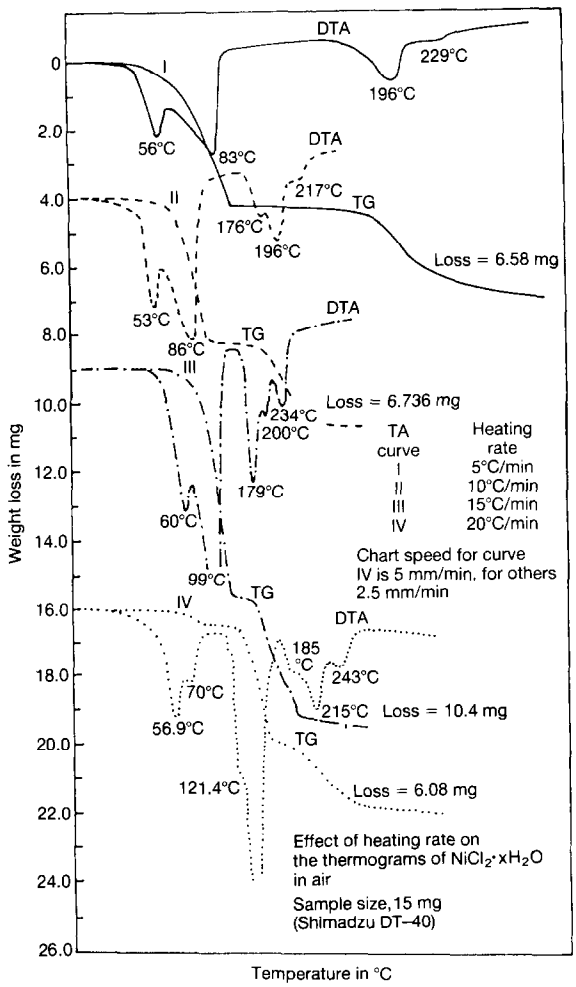

Fig. 2. Thermograms of $NiCl_2 \cdot xH_2O$ obtained using a Shimadzu model DT-40 at different heating rates.

data are given in Table 2. It may be noted from the table that the DTA peak temperature for the first stage of dehydration tends to increase with increase in sample size, a phenomenon that is not apparent for the second and third stages of dehydration. Because liquid and vapour are in equilibrium at any instant in the first stage of dehydration, an increase in sample size produces a higher vapour pressure in the vicinity of the sample and, therefore, the peak temperature shifts to higher values. But the second and third stages of dehydration take place without pre-melting and, therefore, the DTA peak temperatures are independent of sample size. However at higher temperatures and with larger sample sizes, the effect of self-cooling tends to lower the peak temperature by 2–4°C.

TABLE 1

Effect of heating rate on the thermogram of $NiCl_2 \cdot 6.84H_2O$

Rate of heating in °C min^{-1}	DTA peak for initial melting in °C	First stage of dehydration			DTA peak for phase change in °C	Second stage of dehydration			Third stage of dehydration		
		T_i–T_c in °C	DTA peak temp. in °C	Mole of H_2O lost		T_i–T_c in °C	DTA peak temp. in °C	Mole of H_2O lost	T_i–T_c in °C	DTA peak temp. in °C	Mole of H_2O lost
Netzsch (STA-409); sample size, 50 mg											
2	40	60–95	90	3.95	–	155–170	165	1.19	210–240	230	1.09
5	50	90–140	125	3.78	–	170–200	180	1.10	230–270	250	1.19
10	60	90–175	140	4.29	–	175–220	190	0.93	250–300	265	1.23
20	60	110–190	160	4.22	–	190–270	210	1.06	270–340	290	1.20
Shimadzu (DT-40); sample size, 15 mg											
5	56.0	60–90	83.0	3.90	–	148–208	196.5	1.37	220–243	229	1.12
10	53.4	59–110	86.3	4.00	176	185–216	196.0	1.67	216–260	217	0.75
15	54.0	65–135	99.0	4.03	179	190–215	200.4	1.40	215–260	234	0.84
20	50.0	55–140	80.0	3.93	169	180–210	191.0	0.90	210–260	221	1.17

Key: T_i, temperature of inception; T_c, temperature of completion.

TABLE 2

Effect of sample size and nitrogen flow on the thermograms of $NiCl_2 \cdot xH_2O$; heating rate 10°C min^{-1}; Netzsch (STA-409)

Sample size in mg	DTA peak for initial melting in °C	First stage of dehydration			Second stage of dehydration			Third stage of dehydration		
		T_i-T_c in °C	DTA peak temp. in °C	Mole of H_2O lost	T_i-T_c in °C	DTA peak temp. in °C	Mole of H_2O lost	T_i-T_c in °C	DTA peak temp. in °C	Mole of H_2O lost
15.38 [a]	60	90–160	130	4.30	190–250	210	1.70	250–310	270	0.85
29.87 [a]	60	90–160	125	4.21	175–215	190	1.00	240–290	260	1.14
50.23 [a]	60	90–175	140	4.20	175–220	190	0.93	250–300	265	1.23
103.40 [b]	60	125–185	160	4.09	185–220	200	1.21	260–315	280	1.14
99.90 [c]	45	120–175	145	3.12	175–210	190	1.43	250–300	270	1.13
Nitrogen flow, 50 ml min^{-1}										
73.00 [b]	80	100–180	160	4.37	180–220	195	1.06	265–320	280	1.71
101.00 [c]	40	60–175	150	3.16	175–220	190	0.96	250–300	270	1.21

Initial composition of the sample: [a] $NiCl_2 \cdot 6.84H_2O$; [b] $NiCl_2 \cdot 7.55H_2O$; [c] $NiCl_2 \cdot 5.53H_2O$.
Key: T_i, temperature of inception; T_c, temperature of completion.

Effect of inert gas flow

This aspect has been discussed in detail in an earlier paper [2]. The effect of inert gas flow is reflected primarily in the initial melting of the undried sample which shifts to lower temperatures and, consequently, the TG records more loss in weight for the first step of dehydration. However, for partially dried sample containing 5.53 moles of water, a flowing nitrogen environment has practically no effect on the thermogram.

Kinetics of dehydration

The kinetics of dehydration and decomposition from the DTA and TG curves is discussed using two broadly based methods, namely a method independent of any physical model, and a model-dependent integral method. Non-isothermal kinetics is represented by the generalised expression

$$\int_0^{\alpha} \frac{d(\alpha)}{f(\alpha)} = g(\alpha) = \int_0^{T} \frac{A}{b} e^{-E/RT} dT \tag{1}$$

where $g(\alpha)$ is the integral form of $1/f(\alpha)$ which is a function of the mechanism of the thermal process. This may be either a physical model such as nucleation and growth, progress of a reaction interface, diffusional phenomena, etc., or a simple chemical reaction with an order n, i.e. $(1-\alpha)^n$. The right-hand side represents the negative temperature integral function, commonly designated $p(x)$, A and b are the pre-exponential factor of the Arrhenius equation and the heating rate, respectively. Doyle [3] has shown that the ratio $g(\alpha)/p(x)$ is a constant quantity and can be expressed as

$$\log g(\alpha) - \log p(x) = \log \frac{AE}{bR} = B \tag{2}$$

The above equation forms the basis of most of the methods developed so far for the analysis of non-isothermal kinetic data.

Model-independent method

In the absence of any exact solution of the right-hand side of eqn. (1), various approximations have been suggested, the simplest of which was suggested by Doyle himself and is given by

$$\log p(x) = -2.315 - 0.456E/RT \tag{3}$$

Ozawa [4] and also Flynn and Wall [5] have used this expression to solve eqn. (2) for $20 < x < 60$.

Combining eqns. (2) and (3) and rearranging

$$\log b = \log \frac{AE}{Rg(\alpha)} - 2.315 - \frac{0.456E}{RT} \tag{4}$$

If the mechanism of the process does not change with variation in heating rate for a reasonably wide range of α, a plot of $\log b$ versus $1/T$ should yield a series of straight lines for different values of α taken at suitable intervals. From the slope values of these lines, E values can be obtained which are independent of any mechanistic model. This is also known as the "iso-conversion method" of Ozawa, Flynn and Wall (OFW method) [4, 5]. The α values were obtained from the ratio of weight loss at any instant to the total loss in weight at the first broad plateau region at around 350°C in TA curves obtained using the STA-409 apparatus. At the intermediate region of α (0.5–0.6), higher heating rates, e.g. 20°C min^{-1}, result in a deviation from the linear behaviour and, therefore, are not included in the iso-conversion plots (figures not shown).

An examination of the E values obtained from the slopes of the satisfactory linear plots at different α values (see Table 3) reveals the occurrence of at least three stages of water loss. In the range $\alpha = 0.1-0.6$, E values decrease gradually from 32.7 to 25.3 kJ mol^{-1}, but at $\alpha = 0.65$, the E value increases sharply to 109.9 kJ mol^{-1} and then decreases to 92.7 kJ mol^{-1} at $\alpha = 0.75$, corresponding to the loss of 4.73 moles of water. Because the loss of water at $\alpha = 0.6$ is 3.78 moles, the high E value (average, 101.7 kJ mol^{-1}) for the intermediate loss of about 0.95 mole of water possibly involves a structural change in the hydrated salt, as found in the case of the dehydra-

TABLE 3

Activation energy values obtained by the isoconversion method of Ozawa, Flynn and Wall (OFW) and by the DTA peak temperature shift method of Kissinger of the dehydration of $NiCl_2 \cdot xH_2O$

α	Loss of water in mol	OFW		Kissinger
		E in kJ mol^{-1}	Mean E in kJ mol^{-1}	E in kJ mol^{-1}
0.10	0.63	32.8		
0.20	1.26	28.9		
0.30	1.89	28.7		
0.40	2.52	26.7		
0.50	3.15	26.1		
0.60	3.78	25.3	28.1	33.5
0.65	4.10	109.9		
0.70	4.41	102.4		
0.75	4.73	92.7	101.7	71.7
0.80	5.04	80.5		
0.90	5.67	81.4		
0.95	–	76.9		
0.98	6.18	74.0	78.2	67.0

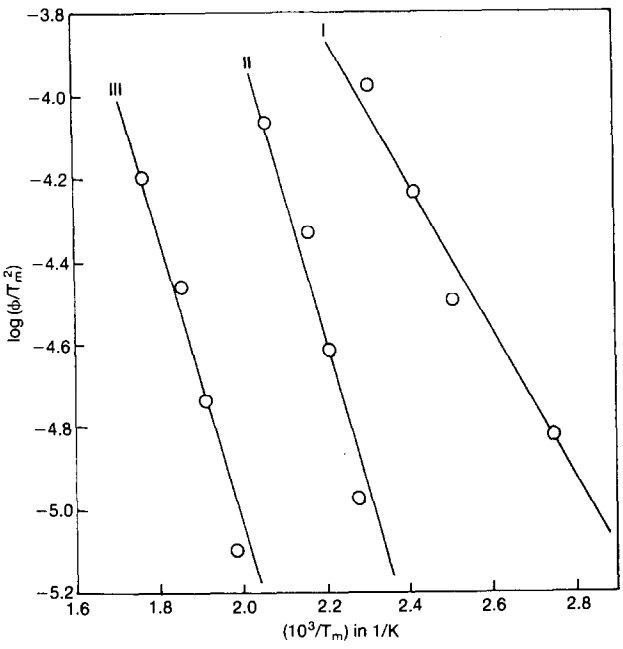

Fig. 3. Kissinger plots for the dehydration of $NiCl_2 \cdot xH_2O$ at different heating rates. Curve numbers denote the different steps of the dehydration.

tion of $CoCl_2 \cdot 6H_2O$ [6]. For the loss of the remaining 1.45 moles of water, a similar mechanism is perhaps operative, as the difference in E values in the range $\alpha = 0.8–0.98$ is small. The average value of E for the first step of dehydration agrees well with that determined from the isothermal method. However, high E values for the other two steps do not agree with those found from either the isothermal or non-isothermal method.

Because in the above method the E value is found to vary with α, an attempt has been made to determine this parameter from DTA traces at different heating rates using the following relationships proposed by Kissinger [7]. Thus when $n = 1$

$$\log\left[\frac{b}{T_m^2}\right] = \log\left[\frac{AR}{E}\right] - \frac{E}{2.3RT_m} \tag{5}$$

and when $n \neq 1$

$$\log\left[\frac{b}{T_m^2}\right] = \log\left\{\left(\frac{AR}{E}\right)n(1-\alpha_m)^{n-1}\right\} - \frac{E}{2.3RT_m} \tag{6}$$

where T_m is the DTA peak temperature and α_m is the conversion at T_m. In either case, the plot of the left-hand side against $1/T_m$ should yield a straight line from the slope of which E can be obtained. Figure 3 shows such plots for the three major endothermic peaks of dehydration obtained using the STA-409; the corresponding E values are shown in Table 3.

Although the E values for the first and third steps are more or less in agreement with those determined from the OFW method, the intermediate step exhibits a lower value.

It has generally been observed that $(1-\alpha_m)$ is almost independent of heating rate and that $n(1-\alpha_m)^{n-1}$ tends to become unity. Therefore, the E value determined by this method is almost independent of n and hence of any mechanistic model.

Model-dependent methods

The following integral methods have been used to derive kinetic parameters from the thermograms of nickel chloride hydrate under different experimental conditions: (i) Horowitz and Metzger (ii) Coats and Redfern, (iii) MacCallum and Tanner, and (iv) Zsako and Zsako. While methods (i) and (ii) are based on the integration of eqn. (1) using the generalised expression for $f(\alpha) = (1-\alpha)^n$, methods (iii) and (iv) are applicable for any mechanistic model, both physical and chemical. It should be stressed here that n is considered as a purely mathematical parameter for describing the kinetics of a thermally stimulated process without any chemical significance, although some of the physical models for decomposition reactions can easily be derived by assuming $n = 0$, 1/2, 1/3, or 1. The basic equations for each method are given below.

(i) Horowitz and Metzger method [8]

$$\log g(\alpha) = \log\left[\frac{1-(1-\alpha)^{1-n}}{1-n}\right] = \frac{E(T_m - T)}{2.3RT_m^2} \tag{7}$$

When $n = 1$

$$\log g(\alpha) = \log[-\ln(1-\alpha)] = \frac{E(T_m - T)}{2.3RT_m^2} \tag{8}$$

where T_m is the temperature (in K) for the maximum rate of conversion. The plot of $\log g(\alpha)$ in eqns. (7) and (8) against $(T_m - T)$ should give the best linear fit for the correct value of n. Knowing E and α_m at T_m, the pre-exponential factor was obtained from eqns. (5) or (6).

(ii) Coats and Redfern method [9]

$$\log\left[\frac{g(\alpha)}{T^2}\right] = \log\frac{AR}{bE}\left[1-\frac{2RT}{E}\right] - \frac{E}{2.3RT} \tag{9}$$

where $g(\alpha)$ is defined in eqns. (7) and (8).

(iii) MacCallum and Tanner method [10]

$$\log g(\alpha) = \log\frac{AE}{bR} - 0.483E^{0.495} - \left[\frac{449+217E}{T}\right] \tag{10}$$

where E is in kcal mol^{-1}; $g(\alpha)$ represents any mechanistic model in its integrated form.

(iv) Zsako and Zsako method [11]. This method is based on the constancy of the right-hand side of eqn. (2) and is assumed to be valid for any reaction model represented by $g(\alpha)$; $p(x)$ is obtained from the empirical formula

$$p(x) = \frac{e^{-x}}{(x+2)(x-d)} \tag{11}$$

where

$$d = \frac{16}{x^2 + 4x + 84}$$

For the calculation of $p(x)$, the E value was varied from 1 to 200 kJ mol^{-1} with intervals of 1 kJ mol^{-1}. For a particular $g(\alpha)$ value, the standard deviation δ for different values of B in the whole range of $p(x)$ values is generally minimised as follows [12]

$$\delta = \left[\frac{\Sigma(B_i - \bar{B})^2}{M}\right]^{1/2} \tag{12}$$

In the above equation, B_i represents the B value calculated from a single point in the TG curve, $\bar{B}$ the arithmetic mean of the individual B_i values, and M the number of experimental points. Zsako and Zsako subsequently [11] used double minimisation, i.e.

$$D_{\bar{m}} = \left[\frac{\Sigma(B_i - \bar{B})^2}{MB^2}\right]^{1/2} \tag{13}$$

The computations for all the different methods of kinetic analysis were performed using an IBM-compatible PC-AT computer by writing suitable programs in BASIC as well as in LOTUS 1-2-3. Each method was made to process data for 22 kinetic models [13, 14]. Because all the output data cannot and need not be presented, we have selected here the "best fit" mechanism for each method based on the highest value of the correlation coefficient r. In the case where more than one mechanism gave close values of r, they are also mentioned for the sake of comparison.

Rate of heating

Table 4 shows the effect of heating rate on the kinetic parameters derived from TG curves from the STA-409 (Fig. 1). It can be seen that for both the first and second stages of dehydration (up to $\alpha = 0.8$) best linear fits are observed with the F_2 mechanism. Only at 10°C min^{-1} does an F_1 or a first-order growth mechanism show slightly higher values of r by the methods (ii), (iii) and (iv). The difference in the standard deviation in method (iv) is so small that F_2 also appears to be just as applicable as F_1. In the case of method (i), the best fit of a model is considered not only from the highest value of r but also from the minimum value of the intercept on the $(T_m - T)$ axis, as eqns. (7) and (8) do not include any intercept.

TABLE 4

Effect of heating rate on the kinetic parameters of the thermal dehydration of $NiCl_2 \cdot xH_2O$; sample size, 50 mg, Netzsch STA-409

Rate of heating in °C min^{-1}	Temp. range in °C	α range	Kinetic model (code)	Horowitz and Metzger			Coats and Redfern			MacCallum and Tanner			Zsako and Zsako		
				E in kJ mol^{-1}	log A in s^{-1}	r	E in kJ mol^{-1}	log A in s^{-1}	r	E in kJ mol^{-1}	log A in s^{-1}	r	E in kJ mol^{-1}	log A in s^{-1}	$D_{\bar{m}}$
First stage															
2	60–100	0.062–0.64	F_2	85.6	10.80	0.93797	80.4	9.83	0.94164	78.2	8.83	0.94902	90.0	11.28	0.0112
5	70–140	0.027–0.621	F_2	80.7	8.46	0.99231	64.4	6.38	0.99407	62.5	5.86	0.99515	65.0	6.46	0.0053
10	80–150	0.030–0.612	F_1	–	–	–	57.2	4.95	0.99763	55.5	4.78	0.99814	64.0	3.26	0.0040
			F_2	78.6	8.17	0.99850	65.8	6.25	0.99724	64.1	6.04	0.99764	73.0	4.50	0.0044
20	110–210	0.013–0.637	F_2	84.1	7.39	0.99536	63.6	4.85	0.99510	61.8	4.96	0.99597	67.0	5.31	0.0059
Second stage															
2	160–180	0.660–0.824	F_2	69.4	6.13	0.98159	63.7	5.86	0.98001	65.4	5.41	0.98372	66.0	6.17	0.0023
5	170–200	0.635–0.803	F_2	49.5	3.39	0.98987	43.0	3.00	0.98885	42.3	2.76	0.99194	44.0	3.15	0.0024
10	180–210	0.064–0.806	F_2	49.7	3.14	0.97551	40.8	2.62	0.96442	40.28	2.71	0.97426	44.0	3.04	0.0041
20	230–260	0.646–0.8	F_2	61.1	3.75	0.97060	51.3	3.24	0.96261	51.7	3.66	0.97233	55.0	3.96	0.0039
Third stage															
2	200–240	0.873–0.985	D_2	–	–	–	–	–	–	13.7	−1.66	0.99180	16.0	−1.15	0.0031
			$F_{1/3}$	12.8	−1.66	0.99225	–	–	–	–	–	–	–	–	–
5	220–260	0.856–0.982	D_1	–	–	–	–	–	–	6.4	−1.94	0.99373	8.0	−2.21	0.0030
			AJ	–	–	–	–	–	–	3.7	−3.25	0.99374	–	–	–
10	230–270	0.843–0.991	D_4	–	–	–	–	–	–	–	–	–	17.0	−2.25	0.0038
			$F_{1/3}$	–	–	–	–	–	–	20.5	−1.04	0.99432	–	–	–
20	280–340	0.830–0.986	D_1	–	–	–	–	–	–	7.3	−1.48	0.98815	–	–	–
			AJ	–	–	–	–	–	–	4.4	−2.79	0.98875	18.0	−1.46	0.0047

The results in Table 4 show that for the first stage of the dehydration, the E value decreases sharply as the rate of heating is increased from 2 to 5°C min^{-1}. From 5 to 20°C min^{-1}, there is no regular trend in the variation of E, suggesting that heating rate has no significant effect on this parameter. For the second stage of dehydration, E values are generally 15–30 kJ mol^{-1} lower than those of the first stage, although the trend in their variation with heating rate is almost similar to that of the first stage. It may also be noted that, except for method (i), the E values obtained from the other three methods show good agreement.

However, for the third stage of dehydration which is better resolved in the thermograms obtained from the STA-409, diffusion appears to be the main rate-controlling mechanism. Low values of activation energy suggest that diffusion takes place through micropores (cracks, fissures, etc.) developed within the bulk of the crystalline phase. These values are in close agreement with those obtained isothermally. It can also be seen that for the last stage of dehydration, comprising a loss of about 13–15%, no single mechanism gives the best fit of the data, either for all four methods or for all the heating rates for a particular method. Thus, E values obtained by method (iv) are considered to be the most representative.

Sample size

Table 5 shows the non-isothermal kinetic parameters with variation in sample size but at a constant heating rate of 10°C min^{-1}. Except for method (iv) which exhibits F_2 mechanism, the other three methods indicate F_1 for the first stage of dehydration of 103.4 mg sample. As the sample size decreases, all four methods suggest the highest correlation coefficients for the F_2 mechanism. However, for the 15.38 mg sample there is some uncertainty with the second stage of dehydration, as more than one mechanism shows equally good correlation coefficients. Perhaps for small amounts of sample, diffusion-controlled processes tend to overlap with an interface growth process. Otherwise, for the second stage of water loss, F_2 appears to be the most appropriate mechanism for a wide range of sample size. As stated in the previous section, no single mechanistic equation can define the last stage of water loss because of the various complex reactions involved. However, low apparent E values (15–20 kJ mol^{-1}) suggest a predominantly diffusion-controlled process. It may be noted from the data in Table 5 that the E values for the first stage of dehydration exhibit a decreasing trend with increase in sample size. This goes rather contrary to the view that the increase in ambient pressure of a gaseous product of a reaction tends to increase the E value. Similarly, for the second stage of dehydration it may be noted that an increase in sample size has little effect on the E values. Perhaps for an interface-growth-controlled mechanism, increase in sample size has little or no effect on the apparent E value.

TABLE 5

Effect of sample size on the kinetic parameters of the thermal dehydration of $NiCl_2 \cdot xH_2O$; heating rate, 10°C; Netzsch STA-409

Sample size in mg	Temp. range in °C	α range	Kinetic model (code)	Horowitz and Metzger			Coats and Redfern			MacCallum and Tanner			Zsako and Zsako		
				E in kJ mol^{-1}	log A in s^{-1}	r	E in kJ mol^{-1}	log A in s^{-1}	r	E in kJ mol^{-1}	log A in s^{-1}	r	E in kJ mol^{-1}	log A in s^{-1}	D_m
First stage															
15.38	80–140	0.023–0.63	F_1	88.2	9.16	0.99395	69.2	6.71	0.99555	67.4	6.49	0.99632	70.0	6.82	0.0041
			F_2	99.4	10.64	0.99644	78.6	8.12	0.99562	76.9	7.89	0.99621	79.0	8.17	0.0041
29.57	90–140	0.046–0.597	F_1	81.6	8.57	0.99626	69.0	6.68	0.99785	67.3	6.47	0.99823	70.0	6.82	0.0024
			F_2	94.2	10.28	0.99856	80.6	8.39	0.99836	79.0	8.16	0.99860	81.0	8.44	0.0021
50.23	80–150	0.030–0.612	F_1	69.1	6.88	0.99636	57.2	4.95	0.99763	55.4	4.77	0.99814	58.0	5.05	0.0032
			F_2	78.6	8.17	0.99850	65.8	6.25	0.99724	64.1	6.04	0.99762	67.0	6.40	0.0036
103.40	110–160	0.133–0.686	F_1	65.0	6.10	0.98601	56.3	4.66	0.97998	54.8	4.56	0.98376	59.0	5.05	0.0069
			F_2	–	–	–	–	–	–	–	–	–	75.0	7.32	0.0065
			$F_{1/3}$		–	–	–	–	–	50.3	3.91	0.98387	–	–	–
Second stage															
15.38	200–230	0.678–0.871	$F_{1/3}$	23.4	−0.23	0.99635	–	–	–	–	–	–	16.0	−1.03	0.0017
			F_1	–	–	–	31.7	1.05	0.99034	31.4	1.24	0.99377	33.0	1.24	0.0019
			D_1	–	–	–	–	–	–	25.4	0.19	0.99615	27.0	0.12	0.0017
29.57	140–220	0.681–0.828	F_1	29.9	0.65	0.98328	–	–	–	20.8	0.15	0.98303	23.0	0.09	0.0033
			F_2	56.3	3.77	0.98330	47.1	3.30	0.97653	46.7	–	0.98256	49.0	3.56	0.0033
50.23	180–210	0.664–0.806	F_1	27.4	0.41	0.97556	–	–	–	–	–	–	21.0	−0.12	0.0041
			F_2	49.7	3.14	0.97551	40.8	2.62	0.96442	40.3	2.71	0.97426	44.0	3.04	0.0041
103.40	170–200	0.700–0.848	F_1	28.0	0.58	0.98038	–	–	–	–	–	–	22.0	0.14	0.0035
			F_2	54.7	3.88	0.98185	46.0	3.49	0.97743	45.3	3.53	0.98325	48.0	3.77	0.0034
Third stage															
15.38	270–290	0.884–0.989	D_1	–	–	–	–	–	–	9.1	−0.78	0.99929	10.0	−2.04	0.0003
			AJ	–	–	–	–	–	–	5.9	−2.91	0.99929	–	–	–
29.57	230–280	0.854–0.985	AJ	–	–	–	–	–	–	–	–	–	14.0	−1.67	0.0018
50.23	230–270	0.843–0.991	$F_{1/2}$	17.4	−1.25	0.99474	–	–	–	–	–	–	17.0	−2.25	0.0038
			D_4	–	–	–	–	–	–	20.5	−1.04	0.99432	–	–	–
103.40	210–270	0.850–0.976	D_2	–	–	–	–	–	–	–	–	–	9.0	−2.15	0.0014

TABLE 6

Isothermal kinetic parameters of dehydration of $NiCl_2 \cdot 5.88H_2O$ in static air and flowing nitrogen environments; heating rate, 10°C min^{-1}

Environment	Temp. range in °C	α range	Kinetic model (code)	Horowitz and Metzger			Coats and Redfern			MacCallum and Tanner			Zsako and Zsako		
				E in kJ mol^{-1}	log A in s^{-1}	r	E in kJ mol^{-1}	log A in s^{-1}	r	E in kJ mol^{-1}	log A in s^{-1}	r	E in kJ mol^{-1}	log A in s^{-1}	D_m
First stage															
Static air (99.9 mg)	110–160	0.085–0.59	F_2	79.7	8.06	0.99478	71.0	6.70	0.99688	69.6	6.53	0.99745	72.0	6.82	0.0027
Flowing N_2 (101.0 mg)	110–160	0.082–0.574	F_1	72.1	6.70	0.99752	58.5	4.84	0.99673	57.1	4.70	0.99726	59.0	4.90	0.0027
			F_2	84.5	8.27	0.99757	–	–	–	–	–	–	–	–	–
			$F_{2/3}$	–	–	–	–	–	–	53.7	4.23	0.99732	–	–	–
Second stage															
Static air	180–210	0.594–0.788	F_1	36.5	1.55	0.96965	–	–	–	27.4	0.88	0.97107	31.0	1.09	0.0045
			F_2	62.9	4.70	0.96985	53.8	4.11	0.96229	–	–	–	58.0	4.63	0.0045
Flowing N_2	180–210	0.595–0.785	F_2	57.1	4.08	0.99243	49.3	3.57	0.99144	48.8	3.61	0.99378	50.0	3.68	0.0021
Third stage															
Static air	220–270	0.802–0.941	D_1	–	–	–	–	–	–	5.27	−1.77	0.99860	7.0	−2.40	0.0029
Flowing N_2	230–280	0.800–0.968	D_1	–	–	–	–	–	–	–	–	–	8.0	−2.80	0.0042
			D_2	–	–	–	–	–	–	3.26	−3.20	0.99430	–	–	–

Inert gas flow

The effect of flowing nitrogen environment on the non-isothermal kinetic parameters of the dehydration of $NiCl_2 \cdot 5.88H_2O$ is shown in Table 6. It may be noted that for the first stage of dehydration the mechansim changes from F_2 in static air to F_1 in flowing nitrogen. For the second stage of dehydration, however, F_2 appears to be the predominant mechanism in both environments. This suggests that the second stage of dehydration (loss of about 1 mole of water) takes place from the solid surface. As expected, the sweeping out of water vapour from near the surface of the reactant tends to reduce the activation energy of the process. Under this circumstance, the rate is predominantly controlled by diffusion of water vapour through the product layer and becomes independent of temperature.

Kinetics of decomposition of the salt above 500°C

The TGA curves of nickel chloride hydrate in the temperature range 500–600°C represent the complex decomposition of the salt to NiO. This step consists of several reactions, including rehydration of the anhydrous salt, dehydrochlorination and dechlorination. Consequently, the kinetic parameters derived for this step are not unique for a particular reaction. However, non-isothermal kinetic parameters have been determined for this step mainly to compare the results with those obtained by isothermal decomposition above 500°C.

The results in Table 7 show that the kinetics of this step in static air appears to be controlled by more than one process, namely diffusional mass transport and progress of reaction interface. However, the isothermal method suggests the interface-progress-controlled mechanism with an order of 1/3 ($F_{1/3}$) and the apparent E value corresponds closely with those obtained by TGA using 100 mg of sample. Here also, the Horowitz and Metzger method shows a higher E value than the other three methods.

In flowing nitrogen environment, the diffusion process (D_1) seems to be the most appropriate rate-controlling step (see Table 7). However, unlike the decomposition in static air, the E value tends to increase by about 1.5 times with the increase in sample size from 73.0 to 101.0 mg. As expected, the E value tends to decrease because of the faster interface growth and, consequently, the diffusion of gaseous product from within the pores becomes rate controlling.

Selection of the suitable method for determination of kinetic parameters from non-isothermal TGA

The mechanism of the major portion of the thermal dehydration of $NiCl_2 \cdot xH_2O$ has been established to be F_2 by both isothermal and non-

TABLE 7

Kinetic parameters for the decomposition (dechlorination) of nickel chloride hydrate in static air and flowing nitrogen environments; Netzsch, STA-409; 10°C min^{-1}

Sample size in mg	Temp. range in °C	α range	Kinetic model (code)	Horowitz and Metzger			Coats and Redfern			MacCallum and Tanner			Zsako and Zsako		
				E in kJ mol^{-1}	log A in s^{-1}	r	E in kJ mol^{-1}	log A in s^{-1}	r	E in kJ mol^{-1}	log A in s^{-1}	r	E in kJ mol^{-1}	log A in s^{-1}	D_m
29.87	560–680	0.206–	D_2	–	–	–	–	–	–	194.4	8.39	0.99977	187.0	7.85	0.0010
(Air)		0.968	$F_{1/3}$	111.6	3.66	0.99919	87.3	2.26	0.99979	94.2	2.75	0.99983	88.0	2.31	0.0007
			$F_{1/2}(R_2)$	121.5	4.25	0.99993	–	–	–	–	–	–	–	–	–
50.23	580–780	0.130–	D_2	–	–	–	–	–	–	164.4	5.80	0.99981	157.0	5.25	0.0012
(Air)		0.991	$F_{1/3}$	–	–	–	71.2	0.86	0.99952	78.8	1.43	0.99965	72.0	0.91	0.0015
			$F_{1/2}(R_2)$	110.9	2.93	0.99907	–	–	–	–	–	–	–	–	–
99.9	600–860	0.091–	D_1	–	–	–	–	–	–	143.1	4.17	0.99984	135.0	3.60	0.0015
(Air)		0.91	$F_{1/3}$	104.6	2.14	0.99913	67.2	0.32	0.99834	75.6	0.92	0.99986	–	–	–
73.0	600–800	0.233–	D_1	–	–	–	–	–	–	98.3	2.14	0.99947	91.0	1.62	0.0019
(N_2 flow)		0.866	$F_{1/3}$	69.5	0.63	0.99959	45.0	−0.72	0.99488	52.8	−0.10	0.99890	47.0	−0.62	0.0023
			$F_{1/2}(R_2)$	74.0	0.92	0.99979	–	–	–	–	–	–	–	–	–
101.0	600–920	0.053–	D_1	–	–	–	–	–	–	138.6	3.34	0.99282	132.0	2.85	0.0107
(N_2 flow)		0.921	$F_{1/3}$	107.2	1.87	0.99537	–	–	–	–	–	–	–	–	–
			AJ	–	–	–	–	–	–	128.4	1.76	0.99537	122.0	1.28	0.0106

TABLE 8

Standard deviations for the variation in the kinetic parameters with experimental conditions for the different methods of kinetic analysis

Methods of kinetic analysis	Effect of heating rate				Effect of sample size					
	First step of dehydration, model F_2		Second step of dehydration, model F_2		First step of dehydration				Second step of dehydration	
					Model F_1		Model F_2		Model F_2	
	E	$\log(A/s^{-1})$	E	$\log(A/s^{-1})$	E	$\log(A/s^{-1})$	E	$\log(A/s^{-1})$	E	$\log(A/s^{-1})$
Horowitz and Metzger	3.182	1.468	9.65	1.375	10.780	1.428	10.820	1.334	3.443	0.399
Coats and Redfern	7.952	2.118	10.371	1.475	7.140	1.100	8.030	1.165	3.365	0.457
MacCallum and Tanner	7.760	1.673	11.450	1.261	7.077	1.051	8.065	1.154	3.364	–
Zsako and Zsako	11.350	3.035	10.532	1.452	6.652	1.022	6.191	0.921	2.646	0.376

isothermal methods. In the case of small sample sizes, because the rate of growth of the interface is slower than the rate of evaporation of water, the kinetic mechanism varies between F_1 and F_2. At temperatures higher than the boiling point of water, the rate of evaporation of water from the freshly crystallised solid surface is so rapid that the diffusion of water molecules through the product layer becomes rate controlling. The kinetic parameters obtained from the four different methods of non-isothermal kinetic analysis are close enough, despite the different assumptions on which they are based. However, a minimum of variation with change in experimental conditions is one of the deciding factors for selecting the most suitable method. Consequently, the standard deviations of the results obtained by each method with variation of either heating rate or sample size are shown in Table 8. It can be noted that as far as the rate of heating is concerned, the Horowitz and Metzger method shows the minimum deviation for both the first and second stages of dehydration. When sample size is varied, the Zsako and Zsako method shows the minimum deviation, irrespective of the mechanism and therefore, this is the most suitable method for both the first and second steps of dehydration. The third, final step of dehydration is not considered, as no definite model-based mechanism is applicable to it.

ACKNOWLEDGEMENTS

The authors thank the Director, R.R.L. Bhubaneswar, for his kind permission to publish this paper. One of the authors (SKM) is grateful to the CSIR, New Delhi for the award of a fellowship.

REFERENCES

1 S.B. Kanungo and S.K. Mishra, Thermochim. Acta, in press.
2 S.K. Mishra and S.B. Kanungo, J. Therm. Anal., 38 (1992) 2417
3 C.D. Doyle, J. Appl. Polym. Sci., 6 (1962) 639.
4 T. Ozawa, J. Therm. Anal., 9 (1975) 369.
5 J.H. Flynn and L.A. Wall, J. Res. Natl. Bur. Std. Sect. A, 70 (1966) 487.
6 J. Ribas, A. Escuer, M. Serra and R. Vincente, Thermochim. Acta, 102 (1986) 125.
7 H.E. Kissinger, J. Res. Natl. Bur. Std., 57 (1966) 217; Anal. Chem. 29 (1959) 1702.
8 H. Horowitz and C. Metzger, Anal. Chem., 55 (1963) 1464.
9 A.W. Coats and J.P. Redfern, Nature, 201 (1964) 68.
10 J.R. MacCallum and J. Tanner, Eur. Polym. J., 6 (1970) 907, 1033.
11 J. Zsako and J. Zsako, Jr, J. Therm. Anal., 19 (1980) 333.
12 J. Zsako, J. Phys. Chem., 72 (1968) 2406.
13 T.P. Bagchi and P.K. Sen, Thermochim. Acta, 51 (1981) 175.
14 J. Sestak and G. Berggren, Thermochim. Acta, 3 (1971) 1.